High-pressure neutron and magnetization investigations of the magnetic ordering in CeSb

T. Chattopadhyay,* P. Burlet, and J. Rossat-Mignod†
Département de Recherche Fondamentale sur la Matière Condensée, Centre d'Études Nucléaires de Grenoble, 38041 Grenoble Cedex 9, France

H. Bartholin
Université de Toulon, 83130 La Garde, France

C. Vettier‡
Institut Laue-Langevin, Boîte Postale 156, 38042 Grenoble Cedex 9, France

O. Vogt
Laboratorium für Festkörperphysik, Eidgenössische Technische Hochschule Zürich, CH-8093 Zürich, Switzerland

(Received 24 January 1994)

High-pressure magnetization and neutron-diffraction experiments have been performed on CeSb under hydrostatic pressure up to 21 kbar in the temperature range 3–32 K. The magnetic ordering in CeSb is very sensitive to hydrostatic pressure. The Néel temperature T_N changes from 16 K at $P=1$ bar to 31 K at $P=21$ kbar. The stability ranges in temperature of the so-called antiferroparamagnetic (AFP) phases decrease continuously with pressure and disappear completely above $P=10$ kbar. At $P=2.5$ kbar, the type-I phase stabilizes at T_N and the transition at T_N crosses over from first to second order giving rise to the critical end point at $P=2.5$ kbar, $T=18$ K. At $P=10$ kbar two phases with magnetic ordering sequences $(++--+-)$ and $(++--+--++-)$ of the ferromagnetic (010) planes are successively observed between type-I and type-IA phases. The results have been discussed in terms of the p-f mixing model.

I. INTRODUCTION

Among cerium compounds, the monopnictides CeX (X=N,P,As,Sb,Bi) show anomalous magnetic properties, especially the heaviest monopnictides, CeSb and CeBi.[1,2] These materials crystallize with NaCl-type ($B1$) structure. The anomalous magnetic properties of the CeBi and CeSb are listed below: (1) The observed values of the crystal-field splitting in the paramagnetic state are unusually small, 37 K in CeSb and 8 K in CeBi.[3] (2) Despite these small values of the crystal-field splitting in the paramagnetic state, the magnetic anisotropies in the ordered phases are extraordinarily large with the easy axis along the [001] direction.[4,5] The anisotropy field, defined as the external magnetic field required to align the magnetization along the [110] direction, has been estimated to be substantially larger than 1000 kOe. (3) Although such a large anisotropy might suggest a large anisotropic exchange interaction, the observed Néel temperatures of CeSb and CeBi (16 and 25 K, respectively) are modest. CeSb shows a first-order transition[6] at T_N, while the transition at T_N in CeBi is second order.[7] (4) Both CeSb and CeBi show complicated magnetic (H,T) phase diagrams.[1,2,8] CeBi shows type-I ordering with the sequence $(+-)$ of the ferromagnetic (001) plane at $T_N=25$ K and type-IA ordering $(++--)$ at $T\simeq T_N/2$ at zero applied field. With magnetic field applied along [001] a ferrimagnetic structure with the sequence $(+++-)$ appears. However, in between type-I and the ferrimagnetic phases and also in between type-IA and the ferrimagnetic phases several long-period structures are observed. The magnetic phase (H,T) phase diagram of CeSb is even more complex and is certainly the most complex ever discovered in any system. There are at least fourteen different phases as shown in Fig. 1. These phases have been classified in Fig. 1 as antiferro- (AF), antiferropara- (AFP), antiferro-

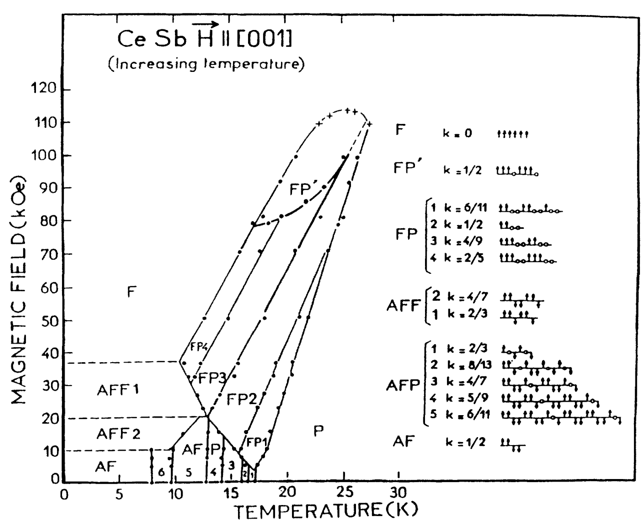

FIG. 1. Magnetic phase diagram of CeSb as a function of temperature and magnetic field applied along [001] direction.

ferro- (AFF), ferro-para- (FP), and ferromagnetic phases and their sequences are also shown in the figure. The most remarkable aspect of these phases is that many of these contain nonmagnetic (or paramagnetic) planes.

These nonmagnetic planes have been claimed to correspond to the dense Kondo state of the Γ_7 level with a small amount of induced moment.[9] Both in CeBi and in CeSb type-IA phase is stabilized at low temperature and at zero applied magnetic field. (5) Short-range magnetic ordering effects have been observed[9,10] both in CeSb and CeBi well above T_N. (6) The observed magnetic anisotropy in the induced magnetic moment at $T=50$ K under a magnetic field of 288 kOe is comparable[11] to that of the ordered state in both CeSb and CeBi. The value of the induced moment at this temperature is about one fifth of the saturation moment. (7) In the paramagnetic state without any external field, the Γ_7 is thought to be the ground level from the susceptibility data,[12] but the results of polarized neutron diffraction performed under 50 kOe of external magnetic field reveal that the main character of the induced moment is that of the Γ_8 state.[13] However, recent studies on $CeSb_{1-x}Te_x$ solutions clearly establish that the crystal-electric-field ground state of CeSb in the paramagnetic state is the Γ_7 doublet.[2] (8) The magnetic excitation spectra have been measured both in CeSb and in CeBi.[14,15] The observed spectra are very similar to each other and the excitation energy is about 4 meV in both cases. The excitations for the wave vectors perpendicular to the ferromagnetic (001) planes are dispersionless indicating a weak interaction between these planes. Even for the wave vectors within the (001) plane the dispersion is weak and has an energy minimum at the [100] zone boundary. This behavior indicates that the couplings of Ce ions on the (001) plane is strongly ferromagnetic in the ground state but is weakly antiferromagnetic when one ion is in the excited state. Such an anisotropic excitation cannot be explained by usual exchange-type interactions.

The origin of the anomalous magnetic properties is not only due to the presence of the $4f$ level close to the Fermi energy (E_F), which is indeed a general feature of anomalous rare-earth systems like those of cerium, but also to the semimetallic character of these cerium compounds. During the past few years extensive calculations have been carried out to explain the complex magnetic properties of CeSb and CeBi by Takahashi and Kasuya[16-21] who have developed the so-called p-f mixing model and by Cooper and co-workers[22,23] who are interested in the consequences of an anisotropic indirect interaction of mixing type as previously derived by Coqblin-Schrieffer using the Schrieffer-Wolf transformation. The p-f mixing model is quite successful in explaining the anomalous magnetic properties of CeSb and CeBi, which according to this model, result from the anisotropic mixing mechanism between the $4f$ states and the valence bands.[16-21] These calculations pointed out the importance of taking into account the symmetry of the $4f$ states (Γ_7 or Γ_8) and of adopting a self-consistent procedure to account for the nonlinear effect arising from the increase in the number of valence holes. The nonlinear effect on the p-f mixing interaction makes the magnetic properties of CeSb very sensitive to an applied hydrostatic pressure via the number of valence holes due to the curvature of the valence hole band. In the present investigation we have studied the effects of hydrostatic pressures on the magnetic properties of CeSb up to 21 kbar by performing high-pressure magnetization and neutron-diffraction experiments. The paper is organized in the following way: In Sec. II we describe the experimental procedures. The (H-T) phase diagram is described in Sec. III. Section IV gives the results of high-pressure magnetization investigations whereas Sec. V gives that of high-pressure neutron investigations. We discuss these results in Sec. VI. Section VII summarizes the results of the present investigations and gives the conclusions arrived at.

II. EXPERIMENTAL

Single crystals of CeSb were grown at E.T.H. Zürich by the recrystallization process described by Busch and Vogt.[24] For high-pressure neutron experiments a single crystal of the size $2\times2\times4$ mm^3 was used. High-pressure neutron-diffraction experiments were performed on the diffractometer DN3 at the Siloé reactor of the Centre d'Etudes Nucléaires in Grenoble. Quasihydrostatic pressures up to 21 kbar were generated by a clamp system designed to be used in a temperature-controlled cryostat. Three different such clamps with slightly different designs and different sizes were used to study the effects of hydrostatic pressure on the many AFP phases of CeSb in different pressure ranges. Liquid C_6F_{14} was used as pressure transmitting medium which also prevented CeSb from reacting with air. The pressures generated were calibrated by measuring the lattice parameter of a NaCl crystal of size of about $2\times2\times2$ mm^3 fixed on top of the CeSb crystal. The diffractometer DN3 is a double-axis diffractometer with a counter arm which can be lifted and therefore allows scans of the nonequatorial reciprocal space up to an angle of 45°. Monochromatic neutrons of two different wavelengths (1.54 and 2.54 Å) were used.

High-pressure magnetization experiments were performed at the Service National des Champs Intenses, Grenoble with the high-pressure, high-field, and low-temperature apparatus. Quasihydrostatic pressures up to 15 kbar were generated by a clamp system under a Cu-Be alloy (Berilco 25) with a cell of sintered alumina WIDALOX. The sample was placed inside an aluminum coated capsule containing the pressure transmitting liquid (1:3 methanol-ethanol) at the center of the cell, between the two pistons in WIDALOX; the seals were made with Be-Cu coated with Cadmium to prevent friction. The pressure was maintained by tightening Be-Cu screws. The pressure was previously applied at room temperature with a standard hydraulic press; the value of pressure obtained at low temperature was deduced from a calibration of the cell by the change of the superconducting temperature of pure lead under pressure in low magnetic field. The cell used for this experiment was 26 mm in outside diameter and had the useful inside diameter of 3.5 mm. The magnetization measurements were performed by the extraction between two opposite pickup coils equipped with compensating coils to reduce the signal due to the pressure cell. Each measurement was corrected for the signal from the pressure cell which was not perfectly compensated. One of the characteristics of the cell was to exhibit a low signal at 4.2 K, whose maximum value is 0.04 emu after compensation at 20 kOe. The sensitivity of the measurements was $\pm 10^{-3}$ emu.

III. MAGNETIC PHASE DIAGRAM OF CeSb AT AMBIENT PRESSURE

Before describing the results of the effects of pressure on the magnetic phase diagram of CeSb,we summarize the results on the magnetic phase diagram of CeSb at ambient pressure.[1,25,26] It is certainly the most complex one discovered so far because it contains, for $H < 70$ kOe, at least fourteen different phases which can be classified into three categories (see Fig. 1):

(i) The antiferro-ferromagnetic phases (AFF) at low temperature $T < 8$ K, correspond to a stacking of ferromagnetic (001) planes with magnetic moments perpendicular to the planes and oriented according to sequences described by square waves of principal wave vector $\mathbf{k}=[00k]$ with $k=\frac{1}{2}$, $\frac{4}{7}$, $\frac{2}{3}$, and 0 as the field is increased. The lines separating these phases are horizontal lines because only a change of magnetization is involved as the magnetic moment is saturated to about $2.06\mu_B$.

(ii) The antiferro-paramagnetic phases (AFP) at low field and high temperature which correspond to a stacking of magnetic and nonmagnetic (001) planes. Below the first-order transition at $T_N=16.2$ K down to 8 K, CeSb undergoes at least five phase transitions. All the corresponding phases are indeed purely antiferromagnetic and commensurate with the lattice; they can be described by square-wave modulations of wave vector $k=n/(2n-1)$ but the phase of the modulation is now locked to give a nonmagnetic layer (P plane) in each period, i.e., every $2n-1$ layers. The distance between nonmagnetic layers becomes larger as the temperature is decreased and transitions are associated only with an entropy variation because the magnetic moments are nearly saturated just below T_N due to the stronger first-order transition; therefore the transition lines are nearly vertical.

(iii) The high-field and high-temperature part of the phase diagram contains the so-called ferro-paramagnetic phases (FP) for which both an entropy and magnetization variations occur at the phase transitions. These FP phases are a unique feature of the phase diagram, they correspond to a stacking of ferromagnetic (001) planes, with a moment of about $2\mu_B$, and nonmagnetic layers with an entropy close to $k_B \ln 2$; actually these nonmagnetic layers exist always by pairs in FP phases whereas they are isolated in AFP phases.

Among the FP phases, the FP2 phase has the most simple stacking $(++00)$ with only two Fourier components of wave vector $k=\frac{1}{2}$ and $k=0$, so no ambiguity exists about the value of the moments in ferromagnetic and in nonmagnetic planes. As an example, for $H=43$ kOe and $T=16$ K, intensity measurements yield the values $m_{\mathrm{Ce}}=2.1\pm0.1\mu_B/\mathrm{Ce}$ and $0.05\pm0.1\mu_B/\mathrm{Ce}$ in ferromagnetic and in nonmagnetic planes, respectively. In order to investigate the very small polarization of cerium magnetic moments within the nonmagnetic planes, neutron experiments have been performed up to $H=100$ kOe on the spectrometer DN3 at the Siloe reactor.[2,27] Surprisingly, the FP2 phase has been observed only in a very narrow temperature range ($24\ \mathrm{K} < T < 25$ K) and for $T < 24$ K in addition to the Fourier components $k=0$ and $k=\frac{1}{2}$ a new component with $k=1$ develops down to $T=19.5$ K where the ferromagnetic state builds up. Therefore in high magnetic fields a new phase, called FP′, exists in the magnetic phase diagram as shown in Fig. 1. Above $H=100$ kOe the border line between the FP′ phase and the paramagnetic state has been determined by magnetization experiments.[2,27] It must be noted that the slope of the transition line between the ferro and the FP′ phases remains the same as for the FP4 phase ($dH/dT=6.3\pm0.5$ kOe/K). Neutron-scattering intensity measurements performed at $H=82$ kOe and $T=17.5$ yield the following values for the Fourier components: $m_{k=0}=1.50\pm0.03\mu_B$, $m_{k=1/2}=0.42\pm0.03\mu_B$, and $m_{k=1}=0.26\pm0.05\mu_B$. Taking into account that the moment value of a cerium ion cannot be larger than $2.14\mu_B$ we get a unique solution which corresponds to the sequence $M'MM'm$ with $M=2.1\pm0.15\mu_B$, $M'=1.7\pm0.1\mu_B$ and $m=0.4\pm0.1\mu_B$. So the FP′ phase can be described approximately by a sequence of three ferromagnetic planes and a single nonmagnetic plane $(+++0)$, a situation which is unique to the FP′ phase. The reduction of the ordered moment in ferromagnetic planes which have a neighboring nonmagnetic plane can be understood only if a strong antiferromagnetic interaction exists between ferro- and nonmagnetic planes. This antiferromagnetic coupling yields also a reduction of the moment in the nonmagnetic planes in comparison with the value reached in the paramagnetic state ($0.4\mu_B$, instead of $0.7\mu_B$ at $H=80$ kOe and $T=25$ K). The large polarization of nonmagnetic planes is reached also in FP phases ($0.35\mu_B$ in the FP2 phase at $T=22.5$ K and $H=82$ kOe), so the very small value observed at $H=43$ kOe must reflect nearly a cancellation in these planes, of the AF exchange by the applied field. In low fields the moments in nonmagnetic planes are actually polarized with a direction opposite to the moments in the ferromagnetic planes as was observed in the FP1 phase [$0.14\pm0.1\mu_B$ at $T=15.7$ K and $H=10$ KOe (Ref. 25)]. In zero field, in the AFP phases, the nonmagnetic planes are isolated and have always two neighboring ferromagnetic planes with an up and down magnetization $(+0-)$ giving an exchange field which cancels and so these planes remain ferromagnetic.

The antiferromagnetic coupling between magnetic and nonmagnetic planes has probably its origin in the p-f mixing and may explain why nonmagnetic planes exist usually by pairs.

IV. RESULTS OF HIGH-PRESSURE MAGNETIZATION EXPERIMENTS

High-pressure magnetization experiments have shown no significant change of saturated magnetic moment with pressure up to about 16 kbar. The moment value $(\sim 2\mu_B)$ corresponds to the saturated moment of the multiplet $J=\frac{5}{2}$. At 4.2 K a small pressure variation of the critical fields corresponding to the appearance of the FP phases containing paramagnetic planes is observed. Figure 2 shows the (P,T) phase diagrams of CeSb at 35 and 51 KOe deduced from magnetization experiments. The FP phases disappear with increasing pressure and are replaced progressively by a FP′ phase. This FP′ phase has already been observed above 80 KOe at the ambient pressure. Recalling the magnetic ordering and magnetic moments in FP and FP′ phases[2] this result indicates that an increase in the magnetic field or in pressure leads to the appearance of a magnetic moment in the paramagnetic planes associated, at the same time, with a decrease of the magnetic moment in the neighboring ferromagnetic planes. The magnetic field necessary to stabilize the FP′ phase decreases as the pressure increases or vice versa—pressure or magnetic field acting in the same way to stabilize the FP′ phase. The effect of the magnetic field is to lower the Γ_8 level whereas the pressure presumably increases the p-f mixing leading to the same effect.

In low field, at ambient pressure, and in increasing temperature the AFP phases disappear in a first-order transition to the paramagnetic phase at T_N. Neutron-diffraction experiments, to be described later, have established that, a higher pressure, a type-I phase appears just below T_N in a second-order phase transition. Although preliminary magnetization experiments[28] missed this type-I phase we have been able to detect this phase during the present investigation. The magnetization experiments confirm clearly that the increase in pressure leads to a change of transition at T_N from first order to second order.

In zero field the ordering temperature strongly increases with pressure especially at low pressures (between 1–3 kbar) where the cross over from the first- to the second-order transition takes place. Therefore, the AF1

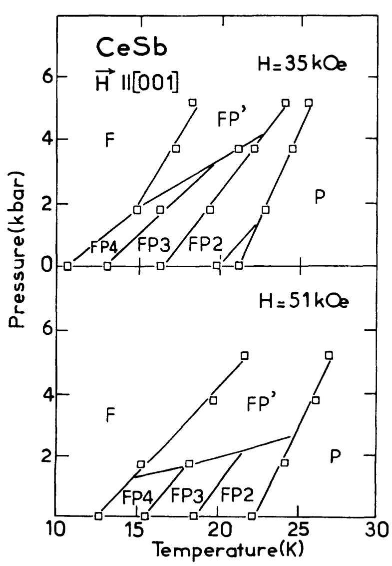

FIG. 2. Magnetic pressure-temperature (P,T) phase diagram of CeSb for magnetic fields of 35 and 51 kOe applied parallel to the [001] direction.

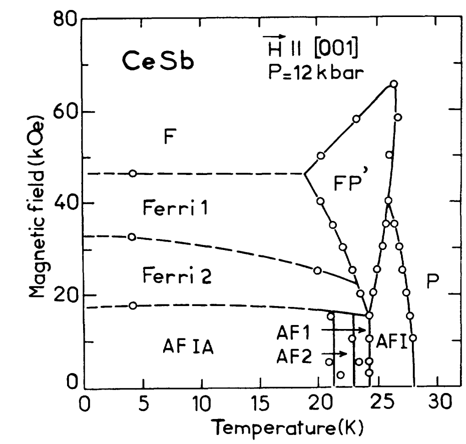

FIG. 3. Magnetic (H,T) phase diagram of CeSb at $P=12$ kbar with the magnetic field applied parallel to the [001] direction.

(type-I) phase is stabilized in CeSb as the first magnetic phase developing below T_N at $P=2.5$ kbar. In order to illustrate the effect of high pressures on the different phases, the (H,T) magnetic phase diagram at $P=12$ kbar is given in Fig. 3. The AFP and the FP phases have disappeared at $P=12$ kbar. The zone occupied by the FP′ phase is much smaller than the zone occupied by the FP phases at the ambient pressure. The stability range of the type-IA phase has increased at higher pressure. Two phases are observed between the type-I and type-IA antiferromagnetic phases in agreement with the results of neutron-diffraction experiments to be described in the next section.

V. RESULTS OF HIGH-PRESSURE NEUTRON-DIFFRACTION EXPERIMENTS AT $H=0$

Figure 4 shows the temperature variation of the intensity of the superlattice peak $[2,k,0]$ at $P=1$ bar and $P=9$ kbar and that of $[1,1,1-k]$ superlattice peak at $P=18$ kbar. The dramatic effect of hydrostatic pressure on the magnetic ordering of CeSb is rather evident from this figure. At $P=1$ bar CeSb undergoes a first-order transition at $T_N=16$ K to the so-called antiferro-para (AFP) phase with $k=\frac{2}{3}$ with the sequence $(+0-+0-)$ where $+,-$, and 0 stand for ferromagnetic (001) planes with spins up and down, 0 signifies a paramagnetic plane, respectively. As the temperature is lowered, transitions to several other AFP phases take place in agreement with the results reported earlier.[29,30] The wave vectors of these AFP phases are $k=\frac{8}{13}, \frac{4}{7}, \frac{5}{9}$, and $\frac{6}{11}$. All these AFP phases contain paramagnetic planes and the sequences of the planes are shown in Fig. 1. At $T=8$ K CeSb undergoes a transition to the type-IA phase ($k=\frac{1}{2}$) with the sequence $(++--)$. These AFP phases are all commensurate phases with wave vectors which follow a general formula $k=n/(2n-1)$ except for the wave vector $k=\frac{8}{13}$. The $k=\frac{1}{2}$ corresponds to $n=\infty$. In addition to the magnetic superlattice peaks associated with the wave

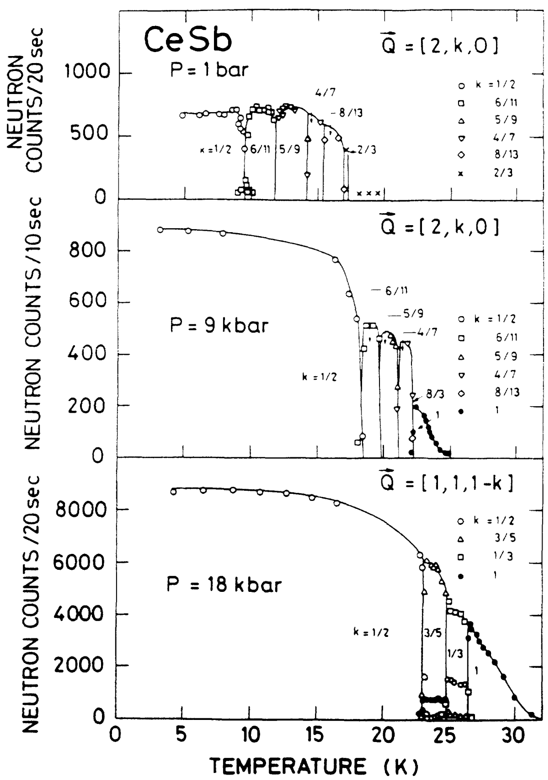

FIG. 4. Thermal variation of the intensity of the superlattice peak $[2,k,0]$ of CeSb at $P=1$ bar and $P=9$ kbar and $[1,1,1-k]$ peak at $P=18$ kbar.

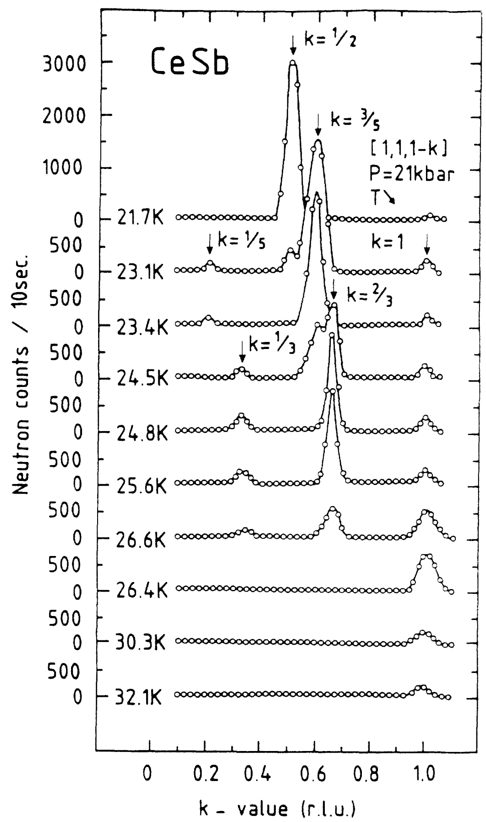

FIG. 5. Reciprocal lattice scans in CeSb along $[00k)$ direction performed in decreasing temperature under an applied pressure 21 kbar.

vector k, small superlattice peaks have been observed which correspond to the third-order harmonics. The magnetic structures of these phases therefore correspond to the square-wave structures with wave-vector values equal to the Fourier component associated with the more intense superlattice peaks. All these results are in agreement with those reported and discussed earlier.[29,30]

As the pressure is increased gradually T_N increases at a rate $dT_N/dP=0.7$/kbar up to about $P=2.5$ kbar. The stability ranges of the AFP phases decrease whereas the stability range of the type-IA phase increases continuously as the pressure is increased. At $P=2.5$ kbar, however, the superlattice peak corresponding to $k=1$ appears at T_N and the transition is found to be second order. As the temperature is lowered the sequence of AFP phases are obtained and finally a type-IA phase is found. The new phase at T_N is the well known type-I phase with the sequence $(+-)$. The appearance of this phase is not surprising. Correlations corresponding to type-I ordering have already been observed in CeSb at $T>T_N$ in critical scattering. The effect of hydrostatic pressure is to convert the short-range order corresponding to the type-I phase into an ordered type-I phase. As the pressure is further increased T_N increases more rapidly. The stability ranges of type-I and type-IA increases whereas the stability ranges of the AFP phases decreases continuously. At about 10 kbar AFP phases disappear completely. Two new commensurate phases appear in between the type-I and type-IA phases and these are called AF1 and AF2 phases. Figure 5 shows reciprocal scans along $[00k]$ direction at $P=21$ kbar, the highest pressure obtained by the present experiments. The structure of the AF1 phase contains the three Fourier components of the wave vector $\mathbf{k}=[00k]$ with $k=\frac{1}{3}$, $k'=2k=\frac{2}{3}$, and $k''=3k=1$. Their amplitudes can be explained (see the Appendix) by assuming a stacking sequence $(++--+-)$ for the ferromagnetic (001) planes which is actually a combination of a type-IA $(++--)$ and a type-I $(+-)$ units. The second commensurate phase AF2 is described by a square wave of wave vector $\mathbf{k}=[00k]$, i.e., described by the three Fourier components with $k=\frac{3}{5}$, $k'=3k=\frac{1}{5}$, and $k''=5k=1$. This corresponds to the purely antiferromagnetic sequence (see the Appendix) $(++--+--++-)$. This sequence is actually the sequence which was missing in the series of AFP phases but in the AF2 phase the nonmagnetic planes do not exist any more.

We have studied the temperature dependence of the integrated intensity at the reciprocal point $[1,1,0]$ corresponding to the wave vector $\mathbf{k}=[001]$ at several pressures to study the cross over from the first-order to the second-order phase transition at T_N and also to detect the phase boundaries of the three high-pressure phases, type-I, AF1, and AF2. These three phases, type I, AF1, and AF2 give rise to different intensities at the reciprocal point $[1,1,0]$ corresponding to their first-, third-, and fifth-order harmonics, respectively. Figure 6 illustrates one of such curve at $P=15$ kbar. The continuous in-

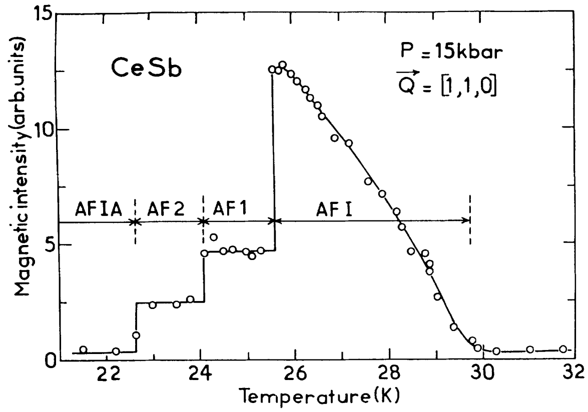

FIG. 6. Intensity of the superlattice peak [1,1,0] of CeSb at $P=15$ kbar as a function of temperature.

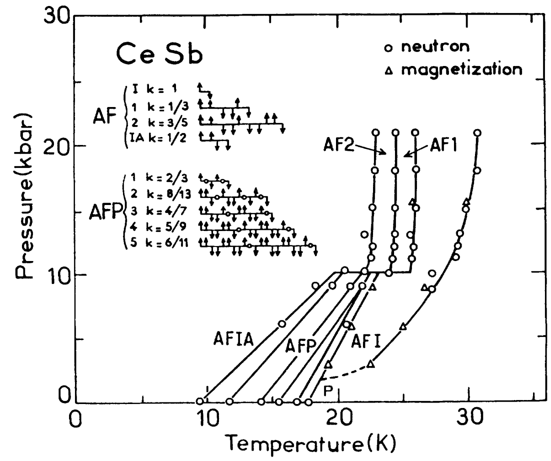

FIG. 8. Magnetic (P,T) phase diagram of CeSb at $H=0$.

crease in intensity, as the temperature is lowered from $T=30$ to $T=26$ K, illustrates the second-order nature of the transition at T_N of the type-I phase. The sudden drops in intensity at about 25.5 and 24 K correspond to the first-order transitions from the type-I to the AF1 phase and from the AF1 phase to the AF2 phase, respectively. The drop in intensity to the background at $T=22.6$ K corresponds to the transition from the AF2 phase to the type-IA phase for which the intensity at the reciprocal point [1,1,0] is zero.

The magnetic moments of Ce atoms was determined only in the range 1 bar–10 kbar. The clamp cell used for generating pressures higher than 10 kbar did not allow the measurement of the (111) nuclear reflections to determine the absolute scale of the magnetic reflections for geometrical reasons. Fundamental reflections such as, (200), (400) could not be used because of the large extinction effects. The magnetic moment obtained at $T=4$ K and $P=1$ bar is $2.1\pm0.1\mu_B$. There is no significant change in the saturation magnetic moment up to $P=10$ kbar. Figure 7 shows the moment variation with temperature at 1 bar and 10 kbar. At $P=10$ kbar the transition at T_N is second order and the maximum moment obtained in type-I phase is about 35% of the saturation moment. However, at the transition $T_1=22$ K from the type-I phase to the AFP1 phase there is a moment jump of about 100%.

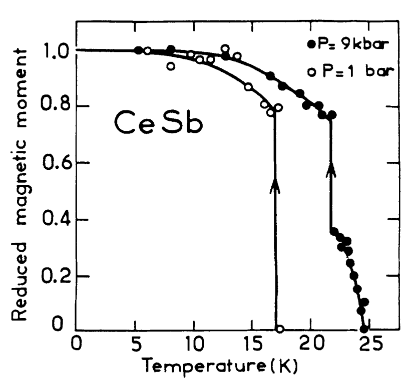

FIG. 7. Reduced magnetic moment of CeSb as a function of temperature at ambient pressure and at $P=9$ kbar. At ambient pressure the transition is of the first order whereas at $P=9$ kbar the transition is of the second order.

Figure 8 shows the pressure-temperature (P,T) phase diagram of CeSb up to $P=21$ kbar. The dramatic effect of pressure on the magnetic phase diagram of CeSb is evident from this diagram. At higher pressures the phase diagram of CeSb is very similar to that for CeBi with the exception that in the former case two commensurate AF1 and AF2 phases exist in between type-I and type-IA phases. The most important result of these high-pressure investigations is the stabilization at about 2.5 kbar of the type-I phase which is observed in critical scattering above T_N. The point P in the (P,T) phase diagram is the so-called critical end point corresponding to $P=2.5$ kbar and $T=18$ K at which a line of critical points corresponding to the second-order phase transitions ends on a line of the first-order transition.

VI. DISCUSSION

A. Magnetic phase diagram of CeSb at ambient pressure

Some theoretical investigations[31–33] have already been performed to explain the complex phase diagram of CeSb by a simple phenomenological one-dimensional axial next-nearest-neighbor Ising model (ANNNI model) and by examining the various phase transitions assuming some sort of exchange interactions between Ce ions. Takhashi and Kasuya[20] have performed a more fundamental microscopic analysis of the magnetic structures of CeSb based on the p-f mixing model. Their calculations predict that the type-IA antiferromagnetic ordering $(++--)$ is the most stable at $T=0$ in zero field both in CeSb and CeBi in agreement with the experimental results. Moreover, the energy of the type-I $(+-)$ structure is a little bit higher than that of the type-IA structure as expected from the experimental results on CeBi. This is also in agreement with our present experimental result of the stabilization of the type-I ordering at T_N in CeSb under a hydrostatic pressure $P \geq 2.5$ kbar and also in agreement with the observation[10] of the fluctuations at $T > T_N$ corresponding to short-range order of the type-I phase in the critical scattering. However, the mechanism which makes type-I structure more stable than type-IA structure at higher temperature is not clear in the calculation. The critical scattering observed in the electrical resistivity[11] near T_N in CeBi suggests the importance of the nesting condition between the conduction electron and the valence hole for the type-I structure. This may also make an important contribution to stabilize the type-I structure near and below T_N. These calculations also show that in the antiferromagnetic structures the holes induced by each character of the $4f$ order are nearly completely confined to each layer because of the very flat dispersion of the resultant valence bands.[20] This is why the various different antiferromagnetic orderings have nearly the same mixing energy.

It has also been shown from these calculations[20] that it is possible for the nonmagnetic planes to coexist with the ferromagnetic planes at a small cost in energy in CeSb, with a fairly large cost in CeBi which is in complete agreement with the experimental results. This is because in CeBi the crystal-field splitting is smaller, while the p-f mixing effect is larger due to a large number of holes (0.06/Ce). These results indicate that an effective interlayer exchange interaction, which can reproduce the present calculation, or the experimentally observed phase diagrams, should be of rather short range. However, the interaction between the nonmagnetic layer and the ordered layer should also be included.

B. Magnetic phase diagram of CeSb at higher pressure

1. First observation of the critical end point in the (P,T) phase diagram of CeSb

Multidimensional critical points such as bicritical, tricritical, tetracritical points, and Lifshitz points in the phase diagrams have been drawing considerable experimental and theoretical interests.[34] Critical end point can be defined as the point where a line of critical points corresponding to the second-order phase transitions ends on line of the first-order phase transitions. Critical end points have been experimentally observed in structural phase transitions. The point P in the (P,T) phase diagram ($P=2.5$ kbar, $T=18$ K) of CeSb represents the observed critical end point in magnetism.[2,29,30] Hälg, Furrer, and Vogt[35] also reports the observation of the critical end point in CeSb under uniaxial pressure. It is to be noted that the critical end point observed under *uniaxial pressure* does not, in principle, belong to the (P,T) phase diagram. The most important result of the present investigation is the stabilization of the type-I phase with a pressure of about 2.5 kbar. Fluctuations corresponding to the antiferromagnetic type-I structure has been already observed[10] above T_N. With decreasing temperature the fluctuations increase as if the system would like to order at about 15 K with the type-I structure, but before the long-range ordering of this structure can occur, the first-order transition to the modulated phase with $k=\frac{2}{3}$ is realized at T_N. Upon dilution for Ce ions, the system $Ce_{1-x}(LaY)_xSb$ successively moves into the type-I regime and for $x=0.3$ an ordinary antiferromagnet with type-I structure with a second-order transition at $T_N \simeq 3$ K is obtained.[36] CeSb is therefore close to the critical conditions for the realization of either a modulated phase with paramagnetic planes and with $k=\frac{2}{3}$ with a first-order transition at T_N or the type-I phase with a second-order transition at T_N. Hydrostatic or (uniaxial) pressure drives the system to the type-I phase with second-order transition at T_N. Hälg and Furrer[15] have shown that CeSb exhibits highly anisotropic magnetic interactions which may be phenomenologically described by bilinear and higher-degree coupling terms. A simple mean-field model for $Ce_{1-x}(La,Y)_xSb$,[36] based on the particular bilinear and higher-degree magnetic interactions of CeSb, illustrates that in this system the bilinear exchange is responsible for type-I ordering and a second-order transition, whereas the higher-order interactions give rise to the modulated structure with paramagnetic planes and first-order transitions.

2. Disappearance of the magnetic phases with paramagnetic planes at P = 10 kbar

The existence of the AFP and FP phases of CeSb in which ferromagnetic and paramagnetic planes coexist is unique. A delicate balance between the crystal-field (CF) splitting Δ and the number of holes in the valence band of the semimetallic CeSb leads to the existence of these paramagnetic planes.[20] Such a severe condition is apparently only fulfilled in pure CeSb. A slight perturbation such as hydrostatic pressure, or the addition of Te leads to the disappearance of these paramagnetic planes.[2]

The p-f hybridization model[20] is quite successful to explain this behavior. In $CeSb_{1-x}Te_x$, addition of Te adds electrons to the conduction band of CeSb and reduces the hole concentration. This reduces the p-f mixing effect responsible for the existence of the paramagnetic planes. Application of hydrostatic pressure increases too much the hole concentration in the conduction band which also leads to the disappearance of the paramagnetic planes in CeSb. Paramagnetic planes do not exist[20] in CeBi because of the too large hole concentration and too small CF splitting.

3. Appearance of the two new high-pressure phases (AF1 and AF2) above P = 10 kbar

At pressure larger than 10 kbar the magnetic ordering in CeSb is very similar to that of CeBi: second-order transition at T_N to a type-I phase and stabilization of the type-IA phase at lower temperature. However, in between the type-I and type-IA phases there exist two new phases AF1 and AF2 in the stacking sequences $(++--+-)$ and $(++--+--++-)$. As in CeBi, paramagnetic planes do not exist any more. The intermediate high-pressure phases AF1 is actually an alternating type-IA and type-I phase where AF2 phase is a mixture of type-I and type-IA phases with stacking faults. Since the energy difference between the type-I and type-IA phases is very small[20] existence of AF1 and AF2 phases in between type-I and type-IA phases is not surprising. At pressures higher than 21 kbar these phases might disappear leading to the high-pressure magnetic ordering in CeSb to be identical with the magnetic ordering in CeBi at ambient pressure.

VII. SUMMARY AND CONCLUSIONS

The present high-pressure magnetization and neutron-diffraction investigations have established that

(1) The type-I phase with the sequence $(+-+-)$, which does not exist in CeSb at ambient pressure, is stabilized by a pressure $P \geq 2.5$ kbar. The magnetic phase transition at the Néel temperature for $P \geq 2.5$ kbar is of the second order. There exists a critical end point in the $(P\text{-}T)$ phase diagram of CeSb at $P=2.5$ kbar and $T=18$ K.

(2) The antiferro-paramagnetic phases (AFP) containing paramagnetic planes disappear for $P \geq 10$ kbar.

(3) At $P \geq 10$ kbar two AF phases, AF1 and AF2 with sequences $(++--+-)$ and $(++--+--++-)$, respectively, are stabilized in between the type-I and type-IA phases.

The above results agree well with the p-f hybridization model.[16–21]

APPENDIX

At high pressure ($P > 10$ kbar) two phases are observed. They include the harmonics of wave vector $\mathbf{k}=[00\frac{1}{3}]$, $\mathbf{k}=[00\frac{2}{3}]$ and $\mathbf{k}=[001]$ and $\mathbf{k}=[00\frac{1}{5}]$, $\mathbf{k}=[00\frac{3}{5}]$ and $\mathbf{k}=[001]$, respectively.

The corresponding magnetic structure must have a periodicity of 3 and 5 unit cells and must correspond to stacking of 6 and 10 ferromagnetic (001) planes, respectively, either up $(+)$ or down $(-)$

The former structure contains all the possible harmonics $\mathbf{k}$, $2\mathbf{k}$, and $3\mathbf{k}$ and consequently it cannot correspond to a square-wave structure because in that case only odd harmonics must exist. This eliminates the sequence $(+++---)$, $(++-++-)$, and $(+0-+0-)$ (AFP phases) and the only remaining possibility is the $(++--+-)$ sequence. The agreement with experiment is easily checked by computing the amplitude $A(k)$ for such a model.

Starting from the general form $A_k = \sum_{R_i} \mathbf{m}(R_i) e^{i\mathbf{k}\cdot R_i}$ one gets with $\mathbf{k}=[00k](2\pi/a)$ and

$$R_i = \left[x,y,z = n\frac{a}{2} \right] 0 < n < 5 \ , \quad x_i, y_i = 0, a/2$$

$$A_k = \sum_n \underset{\sim}{m}(n) \exp i\pi k n \ .$$

For the sequence $(++--+-)$ the A_k are found to be

$$A_{\pm 1/3} = \frac{m_0}{3} \ , \quad A_{2/3} = m_0 i \frac{\sqrt{3}}{3} \ , \quad A_1 = \frac{m_0}{3} \ .$$

The intensities are proportional to $|A_k|^2$ and take the values

$$I(\tfrac{1}{3}) = \frac{m_0^2}{9} \ ,$$

$$I(\tfrac{2}{3}) = \frac{m_0^2}{3} \ ,$$

and $I(1)=m_0^2/9$. The observed intensities are in good agreement with this so that it is proved that the $(++--+-)$ sequences correspond to the real structure.

For the second phase only odd harmonics $[00k]$, $[003k]$, and $[005k]=[001]$ are observed. This implies a square-wave structure. The only possibilities are a $(+++++-----)$ sequence or a $(++--+--++-)$ sequence of the same type as the zero-pressure phase in CeSb of general wave vector $k=n/(2n-1)$. With $n=3$ one gets $k=\pm\frac{3}{5}$, $3k=\pm\frac{9}{5}\equiv\pm\frac{1}{5}$, and $5k=\frac{15}{5}\equiv 1$. The $(+++++-----)$ sequence leads to $k=\frac{1}{5}$ as the fundamental harmonic and to amplitude

$$A(\pm\tfrac{1}{5}) = 0.64 m_0 \ , \quad A(\pm\tfrac{3}{5}) = 0.25 m_0 \ , \quad A(1) = 0.2 m_0 \ ,$$

implying stronger intensity for $k=\frac{1}{5}$ then for $k=\frac{3}{5}$ and $k=1$ in disagreement with the experimental results. The $(++--+--++-)$ sequence leads to the amplitudes

$$A(\tfrac{1}{5}) = 0.25 m_0 \ , \quad A(\pm\tfrac{3}{5}) = 0.64 m_0 \ , \quad A(1) = 0.2 m_0 \ ,$$

which are in good agreement with the experimental results.

---

*Present address: Institute Laue-Langevin, BP156, 38042 Grenoble Cedex, France.

†Deceased.

‡Present address: European Synchrotron Radiation Facilities, BP220, 38043 Grenoble Cedex, France.

[1]Rossat-Mignod, P. Burlet, S. Quézel, J. M. Effantin, D. Delocôte, H. Bartholin, O. Vogt, and D. Ravot, J. Magn. Magn. Mater. **31-34**, 398 (1983).

[2]J. Rossat-Mignod, J. M. Effantin, P. Burlet, T. Chattopadhyay, L. P. Regnault, H. Bartholin, C. Vettier, O. Vogt, D. Ravot, and J. C. Achart, J. Magn. Magn. Mater. **52**, 111 (1985).

[3]A. Heer, A. Furrer, W. Hälg, and O. Vogt, J. Phys. C **12**, 5207 (1979).

[4]G. Busch and O. Vogt, Phys. Lett. **25A**, 449 (1967).

[5]H. Bartholin, D. Florence, W. Tcheng-Si, and O. Vogt, Phys. Status Solidi A **24**, 631 (1974).

[6]B. Lebech, K. Clausen, and O. Vogt, J. Phys. C **13**, 1725 (1980).
[7]F. Hulliger, M. Landolt, H. R. Ott, and R. Schmelczer, J. Low Temp. Phys. **20**, 269 (1975).
[8]H. Bartholin, P. Burlet, S. Quézel, J. Rossat-Mignod, and O. Vogt, J. Phys. Paris **40**, C5-130 (1979).
[9]M. Sera, T. Fujita, T. Suzuki, and T. Kasuya, *Valence Instabilities* (North-Holland, Amsterdam, 1982), p. 435.
[10]B. Hälg, A. Furrer, W. Hälg, and O. Vogt, J. Phys. C **14**, L961 (1981).
[11]T. Suzuki, M. Sera, H. Shida, K. Takegahara, H. Takahashi, A. Yanase, and T. Kasuya, *Valence Fluctuations in Solids* (North-Holland, Amsterdam, 1981), p. 255.
[12]Y. L. Wang and B. R. Cooper, Phys. Rev. B **2**, 2607 (1970).
[13]J. X. Boucherle, A. Delapalme, C. J. Howard, J. Rossat-Mignod, and O. Vogt, Physica B **102**, 253 (1980).
[14]J. Rossat-Mignod, J. M. Effantin, C. Vettier, and O. Vogt, Physica **130B**, 555 (1985).
[15]B. Hälg and A. Furrer, Phys. Rev. B **34**, 6258 (1986).
[16]H. Takahashi and T. Kasuya, J. Phys. C **18**, 2697 (1985).
[17]H. Takahashi and T. Kasuya, J. Phys. C **18**, 2709 (1985).
[18]H. Takahashi and T. Kasuya, J. Phys. C **18**, 2721 (1985).
[19]H. Takahashi and T. Kasuya, J. Phys. C **18**, 2731 (1985).
[20]H. Takahashi and T. Kasuya, J. Phys. C **18**, 2745 (1985).
[21]H. Takahashi and T. Kasuya, J. Phys. C **18**, 2755 (1985).
[22]R. Siemann and B. R. Cooper, Phys. Rev. Lett. **44**, 1015 (1980).
[23]P. Thayamballi, D. Yang, and B. R. Cooper, Phys. Rev. B **29**, 4049 (1984); G. Hu and B. R. Cooper, *ibid.* **48**, 12743 (1993).
[24]G. Bush and O. Vogt, Phys. Lett. **20**, 152 (1962).
[25]J. Rossat-Mignod, P. Burlet, H. Bartholin, O. Vogt, and R. Lagnier, J. Phys. C **13**, 6381 (1980).
[26]J. Rossat-Mignod, P. Burlet, J. Villain, H. Bartholin, W. Tcheng-Si, D. Florence, and O. Vogt, Phys. Rev. B **16**, 440 (1977).
[27]D. Effantin, Ph.D. thesis, University of Grenoble, 1985.
[28]H. Bartholin, D. Florence, and O. Vogt, J. Phys. Chem. Solids **39**, 89 (1978).
[29]T. Chattopadhyay, P. Burlet, J. Rossat-Mignod, H. Bartholin, C. Vettier, and O. Vogt, J. Magn. Magn. Mater. **54-57**, 503 (1986).
[30]T. Chattopadhyay, P. Burlet, J. Rossat-Mignod, H. Bartholin, C. Vettier, and O. Vogt. J. Magn. Magn. Mater. **63&64**, 52 (1987).
[31]J. Böehm and P. Bak, Phys. Rev. Lett. **42**, 122 (1979).
[32]V. L. Pokrovsky and G. Uimin, J. Phys. C **15**, L353 (1982).
[33]J. Villain and M. B. Gordon, J. Phys. C **13**, 3117 (1980).
[34]See, *Multicritical Phenomena,* Vol. 106 of *Nato Advanced Studies Institute, Series B: Physics,* edited by R. Pynn and A. Skjeltrop (Plenum, New York, 1984).
[35]B. Hälg, A. Furrer, and O. Vogt, Phys. Rev. Lett. **57**, 2745 (1986).
[36]B. Hälg, A. Furrer, and O. Vogt, Phys. Rev. Lett. **54**, 1388 (1985).